

Diagnosis of Solid Breast Tumors Using Vessel Analysis in Three-Dimensional Power Doppler Ultrasound Images

Yan-Hao Huang · Jeon-Hor Chen · Yeun-Chung Chang ·
Chiun-Sheng Huang · Woo Kyung Moon ·
Wen-Jia Kuo · Kuan-Ju Lai · Ruey-Feng Chang

Published online: 8 January 2013
© Society for Imaging Informatics in Medicine 2013

Abstract This study aims to evaluate whether the distribution of vessels inside and adjacent to tumor region at three-dimensional (3-D) power Doppler ultrasonography (US) can be used for the differentiation of benign and malignant breast tumors. 3-D power Doppler US images of 113 solid breast masses (60 benign and 53 malignant) were used in this study. Blood vessels within and adjacent to tumor were estimated individually in 3-D power Doppler US images for differential diagnosis. Six features including volume of vessels, vascularity index, volume of tumor, vascularity index in tumor, vascularity index in normal tissue, and vascularity index in surrounding region of tumor within 2 cm were evaluated. Neural network was then used to classify tumors by using these vascular features. The receiver operating characteristic (ROC) curve analysis and Student's *t* test were used to estimate the performance. All the six proposed vascular features are statistically significant ($p < 0.001$) for classifying the breast tumors as

benign or malignant. The A_z (area under ROC curve) values for the classification result were 0.9138. Accuracy, sensitivity, specificity, positive predictive value, and negative predictive value of the diagnosis performance based on all six proposed features were 82.30 (93/113), 86.79 (46/53), 78.33 (47/60), 77.97 (46/59), and 87.04 % (47/54), respectively. The *p* value of A_z values between the proposed method and conventional vascularity index method using *z* test was 0.04.

Keywords 3-D ultrasound · Power Doppler ultrasound · Breast tumor · Vascularity

Introduction

Tumor vascularity is an important factor closely correlated with tumor malignancy [1]. Studies have shown that the

Y.-H. Huang · R.-F. Chang (✉)
Department of Computer Science and Information Engineering,
National Taiwan University,
Taipei, Taiwan 106, Republic of China
e-mail: rfchang@csie.ntu.edu.tw

J.-H. Chen
Tu & Yuen Center for Functional Onco-Imaging,
Department of Radiological Sciences, University of California,
Irvine, CA, USA

J.-H. Chen
Department of Radiology, E-Da Hospital and I-Shou University,
Kaohsiung, Taiwan, Republic of China

Y.-C. Chang
Department of Medical Imaging, National Taiwan University
Hospital and National Taiwan University College of Medicine,
Taipei, Taiwan, Republic of China

C.-S. Huang
Department of Surgery, National Taiwan University Hospital,
Taipei, Taiwan, Republic of China

W. K. Moon
Department of Diagnostic Radiology, College of Medicine,
Seoul National University Hospital,
Seoul, South Korea

W.-J. Kuo
Department of Information Management, Yuan Ze University,
Chung-Li, Taiwan, Republic of China

K.-J. Lai
Department of Computer Science and Information Engineering,
National Chung Cheng University,
Chiayi, Taiwan, Republic of China

R.-F. Chang
Graduate Institute of Biomedical Electronics and Bioinformatics,
National Taiwan University,
Taipei, Taiwan, Republic of China

vascular geometry in malignant tumors was relatively chaotic compared with that in benign tumors [2]. To increase the diagnostic accuracy, morphologic features of tumor vessels have been taken into consideration [3, 4]. Doppler ultrasound could provide a noninvasive method for assessing vessels and is a reliable tool for investigating vascular flow direction and velocity [5, 6]. Holcombe et al. [7] found that malignant tumor is more likely to have detectable flow than benign tumor and when it is presented in small tumor is highly suggestive of malignancy. In a previous research of two-dimensional (2-D) ultrasonography (US) image [8], counting the number of vessel voxels is the most common method to assess vascularity. Wu et al. [8] proposed the vascularity index (V_1), defined as the number of vessel pixels divided by the number of all pixels of the whole tumor in 2-D Doppler US image, to assess the malignant cervical lymphadenopathy and the performance accuracy was 81 %; sensitivity, 78 %; and specificity, 83 %. However, the V_1 was based on the 2-D image and did not take the entire spatial information into consideration and either vascularity or diagnosis result was highly dependent on the selected representative slice. Unlike 2-D US, three-dimensional (3-D) power Doppler US can provide the detailed anatomy of tumor and reveal more precise distribution of vascular morphology [9].

Besides quantification of vessel amounts based on number of pixels or voxels [3, 4, 10], other features based on vessel morphology and tortuosity were also studied [11, 12]. Besides the power Doppler US, Molinari et al. [13] and Schneider et al. [14] analyzed the vascularity of microvessels on the contrast-enhanced ultrasound according to the microbubble-based characteristics. Maheo et al. [15] evaluated the change of vascular structure on the contrast-enhanced ultrasound to predict the response of chemotherapy. However, because in many centers contrast imaging is not available, the use of Doppler images in this study is good and a clear application for such a situation. Because of the heterogeneously growing vessels related to the tumor location, studies have applied several volumes around tumor, divided vessels into different partitions, and then analyzed the vessels individually [9, 16, 17]. The four specific regions around the tumor [16] were used to evaluate vascularity within different volumes, including inside, upper half, 3-mm shell surrounding, and upper half region of 3-mm shell region of radiologist-defined ellipsoid. Based on the same concept, another study [9] used the manually selected region of interest at the first, middle, and last slices of tumor lesion to build a polygon and analyze the vessel networks inside and outside the polygon individually. The sensitivity, specificity, and accuracy could achieve 94, 69, and 81 %, respectively. In the Gokalp's study [17], whether the vessel is in the central part of the tumor, periphery of the tumor region, or penetrating into the tumor or not was used to distinguish the different pathological type of the tumor and

the sensitivity, specificity, positive predictive value (PPV), and negative predictive value (NPV) were 71.8, 81.8, 73.7, and 80.4 %, respectively. These studies [9, 16, 17] confirmed that the related information of vascular features and tumor region could be combined well for classification of breast tumors in 3-D US diagnosis system.

In the current study, the segmented tumor region was applied to separate the vessels into several volumes. After the tumor volumes of interest (VOI) were determined, the specific regions were used to quantify the vascularity inside, outside, and adjacent to the tumor. These specific tumor-related regions have been used [9, 16, 17] to evaluate the vascular degree. Computer-aided diagnosis (CAD) [18–23] then can help to analyze these quantitative vascular features and can assist physicians to differentiate the tumor more effectively. Thus, the purpose of our study was to evaluate the accuracy of neural network analysis of relation between different volumes corresponding tumor region and vascular features at 3-D power Doppler US for the classification of breast tumors.

Materials and Methods

Patients

In this study, the datasets were collected from 113 consecutive patients between June 2008 and June 2009. All the patients who received 3-D power Doppler US before undergoing surgical excision or percutaneous needle biopsy based on suspicious US findings were applied to evaluate the performance of the proposed system. This study was approved by the local ethics committee, and the informed consent was waived for this retrospective study. The malignant lesions were further confirmed by pathology after the 3-D power Doppler US evaluation. The lesions of all patients were pathologically proven by core needle biopsy fine-needle aspiration cytology. A total of 113 solid breast masses (60 benign and 53 malignant) in 107 patients with definitely visualized tumor vessels at 3-D power Doppler US were used to evaluate the performance of the proposed method. The benign cases included 9 fibroadenomas (tumor size; mean±standard deviation, 15.7±5.0 mm), 39 focal fibrocystic changes (14.5±8.9 mm), 5 papillomas (9.8±2.6 mm), and 7 fibroepithelial lesions (11.3±3.7 mm). The malignant lesions included 34 invasive ductal carcinoma (31.2±20.0 mm), 11 ductal carcinoma in situ (28.0±30.6 mm), and 8 invasive lobular carcinoma (15.6±10.5 mm). The sizes of lesions were based on B-mode US.

US Imaging

All US images were acquired with a 3-D power Doppler US scanner (Voluson 730; GE Kretz, Zipf, Austria) and a 6-

12-MHz-dedicated volume transducer. A suitable volume box size determined by a breast radiologist was chosen properly to include the most vessels with amount of normal surrounding breast tissue. Since there were no specific rules to capture the image, larger view including whole tumor region was usually used to observe the vessels surrounding the tumor. In this study, the scan width size was 4.0 cm and the sweep angle was 25–30°. The 3-D volume was obtained by using a curvilinear probe swept mechanically. The three-dimensional volume files were then saved in Cartesian coordinates and observed using the 4D-View program with US scanner.

Image Preprocessing

In general, undue brightness, undue darkness, low contrast, and speckle noises are some common artifacts in ultrasound images. To achieve the purpose of acquiring better segmentation result of tumors in ultrasound gray images, it is necessary to perform a series of image preprocessing operations.

In order to promote the discrimination between region of tumor and region of normal tissue for tumor segmentation, the sigmoid filter [24] was then further used to highlight the boundaries of tumor. For reducing the noise influence, sigma edge-preserving filter [25] was used to smooth image without discarding the tumor boundary information. This filter was to average over the neighboring and similar pixels of each pixel, and these similar pixels was defined as the intensity within the difference of one standard deviation computed from the entire neighborhood. Moreover, in according to the usage of our main segmentation method, level set [26], the magnitude of gradient image [27] were extracted as the input of level set method from the smoothed image. Figure 1b–d shows the preprocessing results of ultrasound image.

Tumor Extraction

Segmentation plays an important role to precisely extract the region of tumor for quantifying the relationship between tumor growth and vascularity. In this study, level set method [26, 28] was used to extract the boundary between tumor voxels and normal tissue voxels. It needed a seed within tumor to construct initial tumor contour and then iteratively modify the contour until it converged. It is a numerical computing algorithm to trail the propagating isosurface step by step. For segmenting the tumor contour, it could start from a 3-D surface and evolve it to approach the zero-level set $\Gamma(x, t) = \{\psi(x, t) = 0\}$ in Fig. 2, where x is a point in \mathfrak{RN} , t is time, and $\psi(\cdot)$ is level-set function. The segmented result of Fig. 1a is shown in Fig. 1e.

Finally, the tumor VOI was segmented and then this result was further used to analyze the relation between tumor and vessels.

Vessel Extraction

In the decoded power Doppler ultrasound vessel image, the colored voxels are represented in red, green, and blue color system. Power Doppler depicted the amplitude of Doppler signals and stores in the color-encoded information that serves as index [29]. The corresponding voxels shown in a power Doppler ultrasound image revealed a brighter red color when the amount of blood flow in vessels increases. Therefore, we applied a predefined threshold value T_R to examine the red channel for each voxel. The voxel in the vessel image will be represented as vascular point if its red component R is equal to or greater than T_R . In this study, the value of T_R is manually selected to be 120 by experienced physicians. Because the vessels with higher blood flow were supposed to more closely correlate with tumor pathologies,

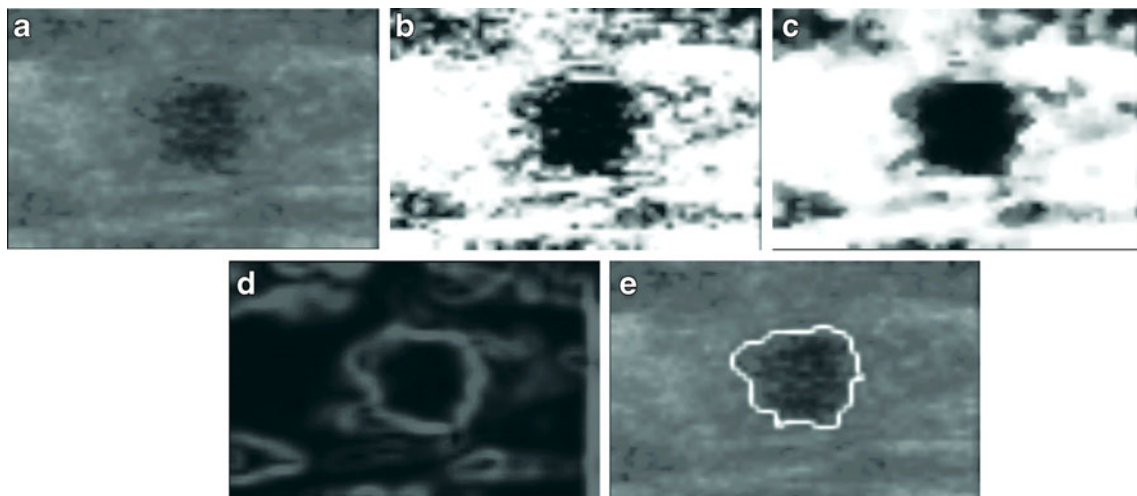


Fig. 1 A segmenting sequence of benign case. **a** Original image. **b** Sigmoid filter result. **c** Sigma filter smooth. **d** Gradient image. **e** The segment result after applying the level set method

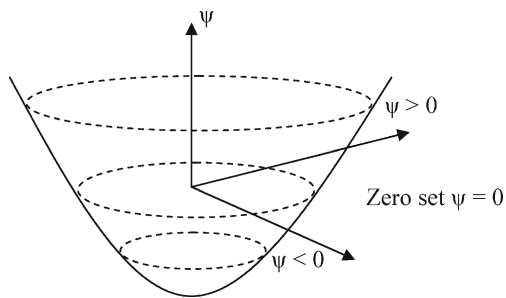


Fig. 2 Zero set in a level set. The sign of ψ is different between inside and outside zero level set

the threshold was applied to retain the vessels with higher blood flow for further analysis and remove the artifacts. The original 3-D image was then converted into binary which represented the vascular information.

Feature Extraction

In this study, two kinds of images including gray images and color images were proceeded individually. The vascular features considered for further breast tumor diagnosis were extracted from the 3-D gray scale and color image. Values of six vascular features of tumors were adopted to evaluate benign and malignant tumors.

These features can be classified into two major categories including vessel features and tumor-vessel features. Vessel volume (V_V) and vascularity index (V_I) were the two vessel features used in this study. The first feature, vessel volume, was determined as the volume of vessel voxels in the processed vessel image. Therefore, vessel volume V_V can be evaluated by

$$V_V = N_V \times p^3 \quad (1)$$

where N_V is the total amount of vessel voxels in the processed vessel image and P is the resolution of the image (millimeter per pixel). It had been reported that the statistically significant increase in vascular points was found on the basis of malignancy and metastases compared with benign tumors. It implicated that the growth of malignant carcinomas was closely related to the formation of blood vessels

from the surrounding tissues [8]. Once the density of vessels becomes noticeably high, it shows a high tendency toward the malignancy. The vascularity index V_I determined as the number of vessel voxels divided by the number of total voxels in the entire volume was used to estimate the density of vessels.

The other kind of features were tumor-vessel features that evaluated using both vessel and tumor information. The tumor-vessel features adopted in this study were tumor volume (V_T), vascularity index in tumor (V_{I_in}), vascularity index in normal tissue (V_{I_out}), and vascularity index in neighboring region outside tumor within 2 cm distance ($V_{I_around_2}$). Moreover, the tumor region should be segmented first to extract the features. The tumor volume V_T is determined by the number of voxels in the VOI which had been segmented in advance. Therefore, tumor volume V_T can be evaluated by

$$V_T = N_T \times p^3 \quad (2)$$

where N_T was the total amount of tumor voxels. To observe the degree of vessel density inside tumor VOI, vascularity index in tumor V_{I_in} was defined as

$$V_{I_in} = N_{VT}/N_T \quad (3)$$

where N_{VT} denoted the number of vessel voxels inside VOI obtained from vessel image with corresponding tumor region. Similarly, the degree of vessel density outside tumor VOI was evaluated by vascularity index in normal tissue V_{I_out} defined as

$$V_{I_out} = N_{VN}/N_N \quad (4)$$

where N_{VN} denoted the number of vessel voxels outside the tumor region and N_N denoted the total number of voxels outside the tumor region.

With the growing of tumor, the formation of blood vessels in the normal tissues surrounding the tumor region may be also influenced. Therefore, vascularity index in neighboring region of tumor within the distance of 2 cm ($V_{I_around_2}$) was considered to evaluate the degree of vessel density in the surrounding region. For obtaining the surrounding region, the distance from each pixel to the boundary could be found in a 2-D distance map [30] and it was extended to 3-D distance map recorded the distance between the tumor surface to each

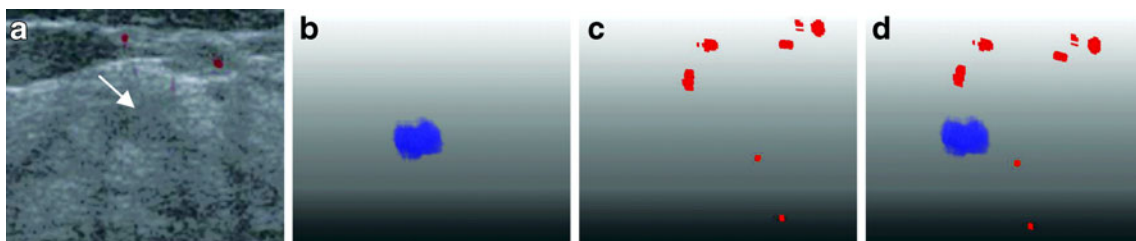


Fig. 3 A benign fibroadenomas case with a tumor size of 10 mm and a predicted value of 0.0163 by using our six features. **a** Original US image with the tumor pointed by the arrow. **b** The segmented 3-D tumor region. **c** The 3-D vascular structure. **d** Components of tumor and vessels

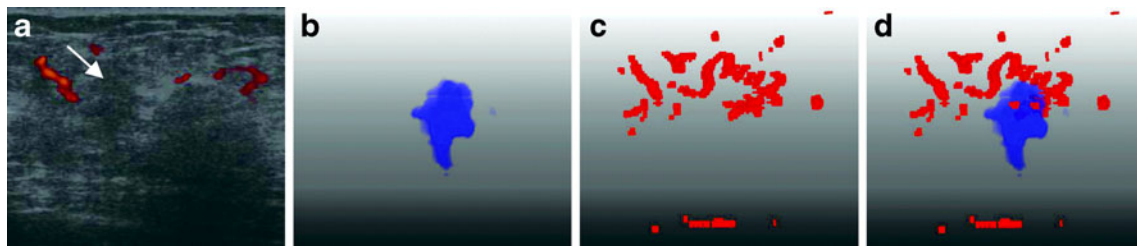


Fig. 4 A malignant invasive ductal carcinoma case with a tumor size of 55 mm and a predicted value of 0.9998 by using our six features. **a** Original US image with the tumor pointed by the arrow. **b** The

segmented 3-D tumor region. **c** The 3-D vascular structure. **d** Components of tumor and vessels

voxel. Due to the different resolution p (in millimeters per pixel) of each image case, the neighbor d millimeter distance we want to focus on could be computed by d/p in voxel distance. In our study, the d distance was 20 mm from the tumor boundary. Vascularity index in neighboring region of tumor $V_{I_around_2}$ was then evaluated by

$$V_{I_around_2} = N_{VA_2} / N_{NA_2} \tag{5}$$

where N_{VA_2} was the number of vessel voxels outside tumor and within 2 cm in the neighboring region and N_{NA_2} was the number of all voxels away from tumor boundary less than 2 cm.

Classification

A general multilayer perceptron neural network with back-propagation learning rule [31] was adopted to classify solid breast tumor based on the values of the proposed six features. The predictive likelihood evaluated by the neural network lies between 0 and 1. A predefined threshold, 0.1, was used to classify the benign and malignant tumors for obtaining a higher sensitivity. The k-fold cross-validation method [32] was used to estimate the performance of the neural network. The 113 3-D power Doppler US images in the database were randomly divided into five groups.

Statistical Analysis

The mean value and standard deviations of the six proposed features were evaluated for benign and malignant tumors by

using 3-D power Doppler US images. Unpaired Student’s t test was used to determine whether the proposed features were statistically significant over the entire database. According to this test, the differences between benign and malignant breast tumors were statistically significant for values of all six features ($p < 0.001$). The performance of the values for these six proposed features was evaluated by receiver operator characteristic (ROC) curve analysis program (LABROC1, 1993; Charles E. Metz MD, University of Chicago, Chicago, IL).

Results

Feature Analysis

In the beginning, tumor extraction algorithm was first applied to extract the tumor VOI. Figures 3 and 4 show the extracted result of VOI for benign and malignant cases which were correctly diagnosed, respectively. In Fig. 5, it shows the VOI of false positive case caused by the too unusual many vessels to result in the benign diagnosis. On the other hand, based on the fewer vessels, it was hard to compute the vascular structure for analyzing the malignant likelihood. A false negative case is shown in Fig. 6. To show the feasibility of six proposed features, the mean value, standard deviation and p value using t test of the six proposed features, V_v , V_l , V_T , V_{I_in} , V_{I_out} , and $V_{I_around_2}$, in benign tumors and malignant tumors are shown in Table 1. Differences between benign and malignant tumors were statistically significant for values of all six proposed features ($p < 0.001$).

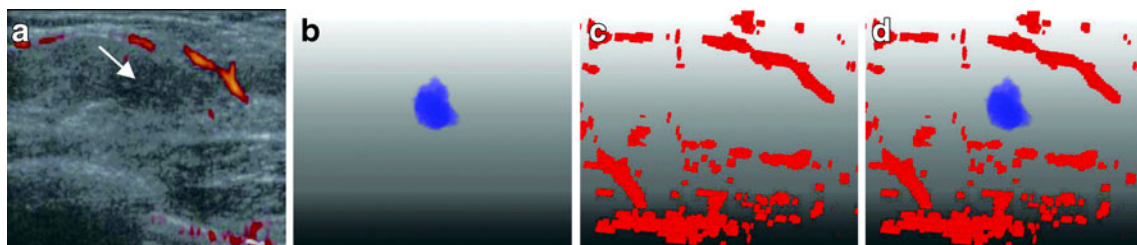


Fig. 5 A false positive case (misdiagnosis) of fibrocystic change with a predicted value of 0.6065 by using our six features. **a** Original US image with the tumor pointed by the arrow. **b** The segmented 3-D tumor region. **c** The 3-D vascular structure. **d** Components of tumor and vessels

Diagnostic Analysis and Accuracy

The ROC area index A_Z over the testing output values was examined to evaluate the overall performance of proposed method. The A_Z value of vessel features— V_V and V_I were 0.93 and 0.83. For the tumor-vessel features— V_T , V_{I_in} , V_{I_out} , and $V_{I_around_2}$, the A_Z values were 0.84, 0.42, 0.82, and 0.81, respectively and show in Fig. 7.

The diagnostic performances of 3-D US image classification results of solid breast tumors using neural network are illustrated in Tables 2 and 3. Accuracy, sensitivity, specificity, PPV, and NPV of the diagnosis performance based on all six proposed features were 82.30 (93/113), 86.79 (46/53), 78.33 (47/60), 77.97 (46/59), and 87.04 % (47/54), respectively. Besides the diagnostic performance of using all features, the diagnostic performances that vascularity index feature, V_I , mentioned before, was used as the only feature for diagnosis were shown in the Table 2 for comparison. In comparison with the proposed scheme, the result using conventional vascular feature, V_I , as the only feature for classification can only achieve 76.99 % accuracy, 84.91 % sensitivity, 70.00 % specificity, 71.43 % PPV, and 84.00 % NPV. Figure 8 illustrates the ROC curves of the neural network classification between benign and malignant tumors using all the proposed features and V_I only. The A_Z values of these two schemes were 0.91 and 0.83, respectively. The corresponding two-tailed p value of these two A_Z values using z test was 0.04.

Discussion

This paper presented a method that quantified the relation between tumor region and blood vessels from 3-D breast power Doppler US images. The quantitative features were further used by CAD system for breast tumor differential diagnosis. The results showed that the proposed neural network method can successfully differentiate breast tumors as benign or malignant with the relation of tumor region and vascular features at 3-D power Doppler US images. The vessel networks could be different functionality with respect to the different tumor regions. In all benign and malignant

Table 1 The mean value, standard deviation, and the p value using t test of six proposed features—vessel volume (V_V), vascularity index (V_I), tumor volume (V_T), vascularity index in tumor (V_{I_in}), vascularity index in normal tissue (V_{I_out}), and vascularity index in around region of tumor ($V_{I_around_2}$) in the benign and malignant tumors ($p < 0.001$)

Value	Type	Mean±standard deviation	p value
V_V	Benign	14.4099±31.6045	<0.001
	Malignant	193.4439±294.6314	
V_I	Benign	0.0010±0.0017	<0.001
	Malignant	0.0045±0.0043	
V_T	Benign	129.2817±119.5978	<0.001
	Malignant	686.6199±822.3662	
V_{I_in}	Benign	0.0002±0.0008	<0.001
	Malignant	0.0022±0.0045	
V_{I_out}	Benign	0.0004±0.0007	<0.001
	Malignant	0.0018±0.0026	
$V_{I_around_2}$	Benign	0.0003±0.0022	<0.001
	Malignant	0.0054±0.0090	

image cases, the majority of vessels were outside tumor. Hence, the vessels outside tumor could reveal the most information of vascular morphology related to the tumor. On the other hand, the malignant tumor was usually with larger lesion size, it would consume much energy to maintain its growing. Hence, the inside-tumor vessel could play an important role to supply nutrition and oxygen to affect the histological changes of tumor tissues [1]. Thus using functional vessel distribution of different region could reflect different tissue characterization and evaluate the malignancy likelihood [9, 16, 17].

The vascularity evaluation at different regions with respect to tumor location was an efficient method to diagnose tumor [9, 16]. The regions formed respectively by the semi-manual polygon [9] and radiologist-defined ellipsoid [16] were confirmed to be useful to quantify vascularity. Compared with other studies [9, 16], our proposed method is unique in terms of the selected regions to evaluate vascularity. In accordance to the functional difference, regions inside, outside and, adjacent to segmented tumor were used to evaluate the vascular features in our study. Compared with the results by using vascularity index feature, accuracy, sensitivity, and specificity of the diagnosis performance

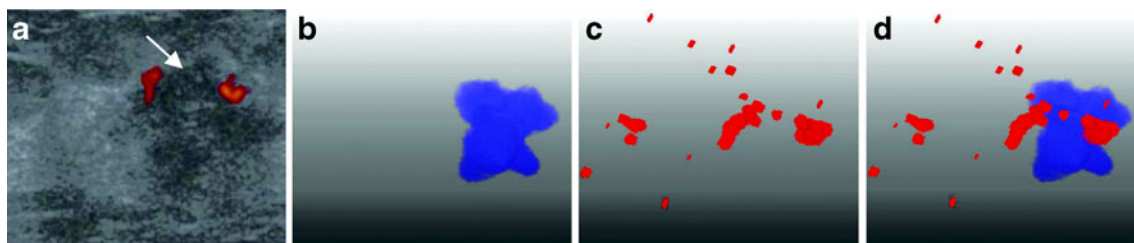


Fig. 6 A false negative case (misdiagnosis) of invasive ductal carcinoma with a predicted value of 0.1002 by using our six features. **a** Original US image with the tumor pointed by the arrow. **b** The segmented 3-D tumor region. **c** The 3-D vascular structure. **d** Components of tumor and vessels

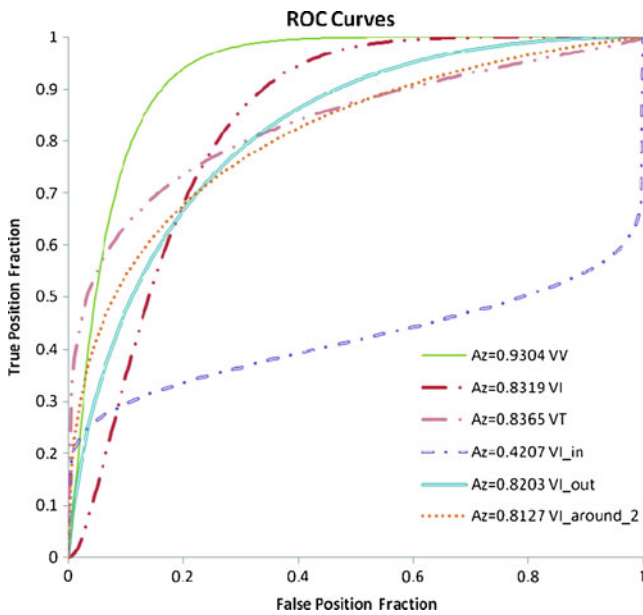


Fig. 7 The ROC analysis of six vascular features

were improved to 82.30 (93/113), 86.79 (46/53), 78.33 % (47/60), respectively.

The qualitative and quantitative analyses based on pixel counts or flow parameters are not superior to the subjective analysis of vessel morphology by radiologists [2, 33]. Therefore, we used the vessel pixel counts as our features and further focused on the quantitative measurements that reflected the vascularity features with corresponding tumor region as depicted by using 3-D power Doppler US [9, 16].

After the tumor region was segmented, the useful features in previous study [8, 10, 11, 34] were applied and incorporated into the tumor region information to extract the vascular properties, tumor-vessel features. Hence, the vessel features related to the tumors were extracted to analyze the tumor, such as blood vessel inside the tumor region, and blood vessel outside the tumor region, and in our study they are useful criteria for differentiating the tumors as malignant or benign. In previous researches [9, 16, 17], the vessels

Table 2 3-D US image classification results of breast tumors using neural network with all proposed features and V_I , respectively

Sonographic classification	NN with all features		NN with V_I	
	Benign ^a	Malignant ^a	Benign ^a	Malignant ^a
Benign	TN 47	FN 7	TN 42	FN 8
Malignant	FP 13	TP 46	FP 18	TP 45
Total	60	53	60	53

TP true positive, TN true negative, FP false positive, FN false negative

^a Histological finding. Accuracy=(TP+TN)/(TP+TN+FP+FN); sensitivity=TP/(TP+FN); specificity=TN/(TN+FP); positive predictive value=TP/(TP+FP); negative predictive value=TN/(TN+FN)

Table 3 Performance indices using neural network with all proposed features and V_I , respectively

Item	All feature (%)	V_I (%)
Accuracy	82.30	76.99
Sensitivity	86.79	84.91
Specificity	78.33	70.00
PPV	77.97	71.43
NPV	87.04	84.00

PPV positive predictive value, NPV negative predictive value

were separated into several partitions to evaluate vascularity, but they only applied the simplest characteristics to diagnose tumor, the accuracy, sensitivity and specificity in the study [17] were only 77.6, 71.8, and 81.8 %, respectively. In our study, the spatial domain was separately into several regions, inside tumor, outside tumor, and the periphery of inside tumor, and then these regions were used to compute vascularity based on vascularity index [8]. The vascular network can be estimated individually with corresponding different tumor region to recognize the tumor malignancy. By exploiting the proposed tumor-vessel features, a higher accuracy can be achieved in comparison with using conventional vessel features as description in Tables 2 and 3. From these two tables, using tumor contour information to evaluate individually the distribution of vessels inside and adjacent to tumor results in a better diagnosis accuracy in our study. The simpler vascular features with tumor region information in

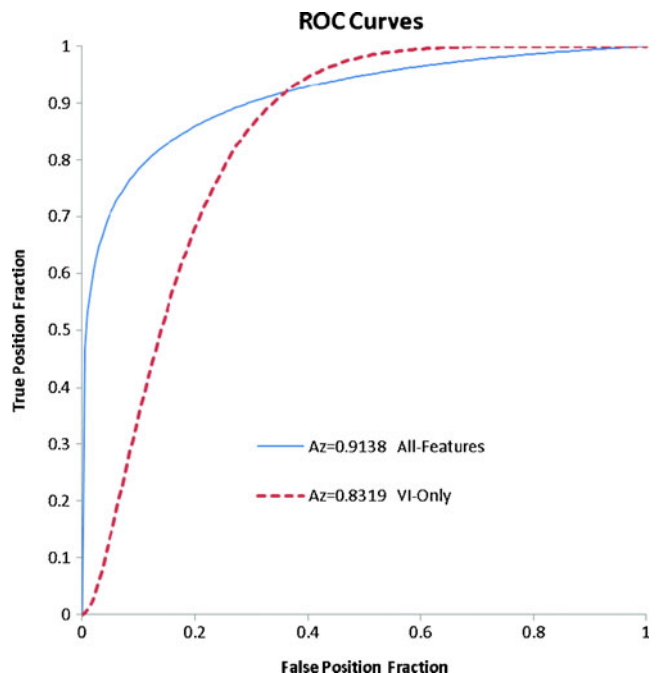


Fig. 8 The ROC analyses of neural networks using all six proposed features and V_I feature only

this research perform as well as Chang's study [11], with experiment accuracy of 85.20 and 84.6 % individually.

Because the number of vessel pixels was decided by the T_R , the extracted features could be affected by this threshold. In the future, the diagnostic accuracy of our system can be improved focusing on three issues. Firstly, the automatic T_R selection algorithm should be further investigated to make the proposed system more robust without manual interference. Secondly, B-mode image could be used not only for segmenting tumor but also for extracting more tumor characteristics [35, 36] to remove the manual influence. Thirdly, more morphological features can be extracted around the tumor region to have more understanding of the relation between vascularity and the likelihood of tumor malignancy. Finally, our vascular features might also be used as prognostic markers to differentiate different histology [37, 38].

In conclusion, we proposed a method that makes use of quantitative relationship between tumor region and vascularity features from 3-D breast power Doppler US images to classify solid breast tumors as benign or malignant. The results showed that 3-D power Doppler US images, combined with computer-aided analysis, can effectively classify benign and malignant breast tumors using the six proposed features with accuracy and sensitivity, 82.30 and 86.79 %.

Acknowledgments The authors thank the National Science Council (NSC 96-2221-E-002-268-MY3), Ministry of Economic Affairs (100-EC-17-A-19-S1-164), and Ministry of Education (AE-00-00-06) of the Republic of China for the financial support.

References

- Gupta MK, Qin RY: Mechanism and its regulation of tumor-induced angiogenesis. *World J Gastroenterol* 9:1144–1155, 2003
- Stuhrmann M, Aronius R, Schietzel M: Tumor vascularity of breast lesions: potentials and limits of contrast-enhanced Doppler sonography. *Am J Roentgenol* 175:1585–1589, 2000
- Hsiao YH, Kuo SJ, Liang WM, Huang YL, Chen DR: Intra-tumor flow index can predict the malignant potential of breast tumor: dependent on age and volume. *Ultrasound Med Biol* 34:88–95, 2008
- Sehgal CM, Arger PH, Rowling SE, Conant EF, Reynolds C, Patton JA: Quantitative vascularity of breast masses by Doppler imaging: regional variations and diagnostic implications. *J Ultrasound Med* 19:427–440, 2000
- Strano S, Gombos EC, Friedland O, Mozes M: Color Doppler imaging of fibroadenomas of the breast with histopathologic correlation. *J Clin Ultrasound* 32:317–322, 2004
- Germer U, Tetzlaff A, Geipel A, Diedrich K, Gembruch U: Strong impact of estrogen environment on Doppler variables used for differentiation between benign and malignant breast lesions. *Ultrasound Obstet Gynecol* 19:380–385, 2002
- Holcombe C, Pugh N, Lyons K, Douglasjones A, Mansel RE, Horgan K: Blood-flow in breast-cancer and fibroadenoma estimated by color Doppler ultrasonography. *Br J Surg* 82:787–788, 1995
- Wu CH, Hsu MM, Chang YL, Hsieh FJ: Vascular pathology of malignant cervical lymphadenopathy: qualitative and quantitative assessment with power Doppler ultrasound. *Cancer* 83:1189–1196, 1998
- Huang YL, Kuo SJ, Hsu CC, Tseng HS, Hsiao YH, Chen DR: Computer-aided diagnosis for breast tumors by using vascularization of 3-D power Doppler ultrasound. *Ultrasound in Med & Biol* 35:1607–1614, 2009
- Kettenbach J, Helbich TH, Huber A, Zuna I, Dock W: Computer-assisted quantitative assessment of power Doppler US: effects of microbubble contrast agent in the differentiation of breast tumors. *Eur J Radiol* 53:238–244, 2005
- Chang RF, Huang SF, Moon WK, Lee YH, Chen DR: Solid breast masses: neural network analysis of vascular features at three-dimensional power Doppler US for benign or malignant classification. *Radiology* 243:56–62, 2007
- Huang SF, Chang RF, Moon WK, Lee YH, Chen DR, Suri JS: Analysis of tumor vascularity using three-dimensional power Doppler ultrasound images. *IEEE Trans Med Imaging* 27:320–330, 2008
- Molinari F, Mantovani A, Deandrea M, Limone P, Garberoglio R, Suri JS: Characterization of single thyroid nodules by contrast-enhanced 3-D ultrasound. *Ultrasound Med Biol* 36:1616–1625, 2010
- Schneider M, et al.: Use of intravital microscopy to study the microvascular behavior of microbubble-based ultrasound contrast agents. *Microcirculation* 19:245–259, 2012
- Maheo K, et al.: Non-invasive quantification of tumor vascular architecture during docetaxel-chemotherapy. *Breast Cancer Res Treat* 134:1013–1025, 2012
- LeCarpentier GL, et al.: Suspicious breast lesions: assessment of 3D Doppler US indexes for classification in a test population and fourfold cross-validation scheme. *Radiology* 249:463–470, 2008
- Gokalp G, Topal U, Kizilkaya E: Power Doppler sonography: anything to add to BI-RADS US in solid breast masses? *Eur J Radiol* 70:77–85, 2009
- Chang RF, Wu WJ, Moon WK, Chen DR: Improvement in breast tumor discrimination by support vector machines and speckle-emphasis texture analysis. *Ultrasound Med Biol* 29:679–686, 2003
- Chen WM, Chang RF, Moon WK, Chen DR: Breast cancer diagnosis using three-dimensional ultrasound and pixel relation analysis. *Ultrasound Med Biol* 29:1027–1035, 2003
- Drukker K, Giger ML, Horsch K, Kupinski MA, Vyborny CJ, Mendelson EB: Computerized lesion detection on breast ultrasound. *Med Phys* 29:1438–1446, 2002
- Drukker K, Giger ML, Vyborny CJ, Mendelson EB: Computerized detection and classification of cancer on breast ultrasound. *Acad Radiol* 11:526–535, 2004
- Horsch K, Giger ML, Venta LA, Vyborny CJ: Computerized diagnosis of breast lesions on ultrasound. *Med Phys* 29:157–164, 2002
- Kuo WJ, Chang RF, Moon WK, Lee CC, Chen DR: Computer-aided diagnosis of breast tumors with different US systems. *Acad Radiol* 9:793–799, 2002
- Suri JS, Kathuria C, Chang R-F, Molinari F, Fenster A: *Advances in Diagnostic and Therapeutic Ultrasound Imaging*. Norwood, MA: Artech House, 2008
- Lee JS: Digital image smoothing and the sigma filter. *Computer Vision Graphics and Image Processing* 24:255–269, 1983
- Malladi R, Sethian JA, Vemuri BC: Shape modeling with front propagation—a level set approach. *IEEE Trans Pattern Anal Mach Intell* 17:158–175, 1995
- Gonzalez RC, Woods RE: *Digital Image Processing*. Englewood Cliffs: Prentice-Hall, 1992
- Osher S, Sethian JA: Fronts propagating with curvature-dependent speed—algorithms based on Hamilton–Jacobi formulations. *J Comput Phys* 79:12–49, 1988
- Wu MH, Tsai SJ, Pan HA, Hsiao KY, Chang FM: Three-dimensional power Doppler imaging of ovarian stromal blood flow in women with endometriosis undergoing in vitro fertilization. *Ultrasound Obstet Gynecol* 21:480–485, 2003

30. Jain AK: Fundamentals of Digital Image Processing. Englewood Cliffs: Prentice-Hall, 1989
31. Haykin S: Neural Networks: A Comprehensive Foundation. Upper Saddle River: Prentice-Hall, 1999
32. Lendasse A, Wertz V, Verleysen M: Model selection with cross-validations and bootstraps—application to time series prediction with RBFN models. *Artificial Neural Networks and Neural Information Processing-Ican/Iconip 2003* 2714:573–580, 2003
33. Schroeder RJ, et al.: D-galactose-based signal-enhanced color Doppler sonography of breast tumors and tumor-like lesions. *Invest Radiol* 34:109–115, 1999
34. Carson PL, et al.: 3-D color Doppler image quantification of breast masses. *Ultrasound Med Biol* 24:945–952, 1998
35. Shen WC, Chang RF, Moon WK, Chou YH, Huang CS: Breast ultrasound computer-aided diagnosis using BI-RADS features. *Acad Radiol* 14:928–939, 2007
36. Shen WC, Chang RF, Moon WK: Computer aided classification system for breast ultrasound based on breast imaging reporting and data system (BI-RADS). *Ultrasound Med Biol* 33:1688–1698, 2007
37. Bhooshan N, Giger ML, Jansen SA, Li H, Lan L, Newstead GM: Cancerous breast lesions on dynamic contrast-enhanced MR images: computerized characterization for image-based prognostic markers. *Radiology* 254:680–690, 2010
38. Bahri S, Chen JH, Yu HJ, Kuzucan A, Nalcioglu O, Su MY: Can dynamic contrast-enhanced MRI (DCE-MRI) predict tumor recurrence and lymph node status in patients with breast cancer? *Ann Oncol* 19:822–U822, 2008